Arch. Mech., **58**, 1, pp. 93–123, Warszawa 2006

Modelling of anisotropic damage by microcracks: towards a discrete approach

R. BARGELLINI, D. HALM, A. DRAGON

Laboratoire de Mécanique et de Physique des Matériaux, UMR CNRS 6617
Ecole Nationale Supérieure de Mécanique et d'Aérotechnique
BP 40109, 86961 Futuroscope Chasseneuil Cedex, France

Modelling of anisotropic damage by microcracks remains a pivotal topic of Damage Mechanics. Many models are built employing a single second-order tensor damage variable $\mathbf{D}$ and its spectral decomposition. However, some inconveniences are encountered such as non-uniqueness of the free energy or decomposition of the strain tensor. This paper first reconsiders the anisotropic damage definition; a discrete approach, which introduces nine microcrack densities associated with nine *fixed* directions, is presented. This definition permits to represent essential phenomena concerning quasi-brittle materials behaviour: the induced anisotropic degradation of elastic properties and the unilateral effect are notably described. In addition, the quoted inconveniences are avoided.

1. Introduction

Quasi-brittle materials such as concrete and rocks, by their nature, contain – independently of their frequent multiphase microstructure (e.g. aggregate and paste in concrete) – numerous inhomogeneities of different types (microcracks, cavities, inclusions...), even before any loading. Their behaviour is principally affected by the growth of pre-existing microcracks and the nucleation of new ones; the development and coalescence of distributed cracks finally lead to fracture at low strain level. Despite the publication of a great number of papers focusing on damage by microcracking during the last thirty years, this subject remains a pivotal topic in the field of Damage Mechanics. Among the difficulties encountered, one may mention:

(i) *the induced anisotropy*: microcracks orientation depends on the loading path; their normals are predominantly oriented, as explained in Sec. 4, in the direction of maximal tension; consequently, when subjected to axial compression, quasi-brittle materials fail by axial splitting; under tension loading, a specimen splits perpendicularly to the tension axis (Fanella and Krajcinovic, [1]);

(ii) *three-dimensional* effects, such as the volumetric dilatancy;

(iii) the crack closure effect (known as "*unilateral effect*") and its consequences, such as recovery of some elastic properties.

Many methods have been used to model these phenomena, either micromechanical or 'macroscopic', although frequently based on micromechanical works (see Krajcinovic [2] for an exhaustive synthesis). However, certain models were essentially two-dimensional (Andrieux *et al.* [3]) while others led to mathematical inconsistencies, in particular when unilateral effect was taken into account, as shown by Chaboche [4] (non-symmetric stiffness, discontinuity of stress-strain response, non-convex reversibility domain …).

During the 90's, some models found a compromise between a thrifty formulation and a physical motivation. One of them was proposed by Dragon *et al.* [5]. A specific thermodynamic framework, based on partitioning of the damage thermodynamic (driving) force was put forward. The main features of the model are the following: it is built by employing a single damage, second-order variable $\mathbf{D}$. As any second-order tensor, $\mathbf{D}$ can be decomposed on its spectral basis: $\mathbf{D} = \sum_{k=1}^{3} D_k \boldsymbol{\nu}_\mathbf{k} \otimes \boldsymbol{\nu}_\mathbf{k}$ where D_k and $(\boldsymbol{\nu}_\mathbf{1}, \boldsymbol{\nu}_\mathbf{2}, \boldsymbol{\nu}_\mathbf{3})$ are the eigenvalues and eigenvectors of $\mathbf{D}$. The damage configuration is then equivalent, in its effects, to a network of 3 orthogonal systems of parallel microcracks. A relevant thermodynamic potential (specific free energy) is proposed; its $\mathbf{D}$-derivative gives the thermodynamic force (affinity) associated to damage, which represents damage energy release rate.

To describe properly the anisotropic damage evolution, the thermodynamic force is split into two parts; one corresponds to the recoverable energy, the other to 'blocked' effects; the latter is further decomposed into two parts corresponding to positive and negative strain ($\boldsymbol{\varepsilon}^+$ and $\boldsymbol{\varepsilon}^- = \boldsymbol{\varepsilon} - \boldsymbol{\varepsilon}^+$). The elastic domain is defined with the former term.

The potential was then enriched in order to describe other phenomena and in particular the unilateral effect by the addition of a closure term (see Halm and Dragon [6] or Dragon and Halm [7]). The term sensible to closure/opening of microcracks comprises a fourth-order tensor formed with the eigenvectors $\boldsymbol{\nu}_k$ and eigenvalues D_k of the second-order tensor $\mathbf{D}$. This term cancels the material stiffness degradation in the $\boldsymbol{\nu}_k$ direction when microcracks normal to $\boldsymbol{\nu}_k$ are closed, namely when:

$$\boldsymbol{\nu}_k . \boldsymbol{\varepsilon} . \boldsymbol{\nu}_k \leq 0. \tag{1.1}$$

Consequently, the spectral decomposition of $\mathbf{D}$ plays a major role in the description of unilateral damage effect in this model.

However, several problems were detected recently; for example:

(i) *The strain tensor decomposition* into a positive and a negative parts leads to inconsistencies : due to the non-dissipative nature of microcrack closure-re-opening (for a fixed state of damage), the recovery formulation should conserve energy. However Carol and Willam [8] show that whatever the projection operators used, formulations that decompose strain (or stress) tensor in the thermodynamic potential (for example ORTIZ [9] or JU [10]) exhibit a spurious dissipation when anisotropic degradation is considered. This drawback comes from the fact that stress stems from differentiation of the thermodynamic potential with respect to total strain while free energy, depending on a part of $\boldsymbol{\varepsilon}$ (namely $\boldsymbol{\varepsilon}^+$ or $\boldsymbol{\varepsilon}^-$), represents a shaky formulation. The corresponding differentiation (with respect to $\boldsymbol{\varepsilon}$) is rigorous only if $\boldsymbol{\varepsilon}^+$(or $\boldsymbol{\varepsilon}^-$) matches $\boldsymbol{\varepsilon}$; in other cases, it appears clumsy.

(ii) *The non-negativity of the dissipation* depends on restrictions on the values taken by the material parameters and the damage variable; for some extreme loading paths, the dissipation may lose its necessary positivity.

(iii) *The free energy may not be* unique in specific configurations (see CORMERY and WELEMANE [11]): the closure term (in HALM and DRAGON [6]) is defined from the eigenvectors of the damage variable $\mathbf{D}$. However, this spectral decomposition can be non-unique (in the case of isotropic damage for example): a given state $(\boldsymbol{\varepsilon}, \mathbf{D})$ can be associated with different values of the free energy. Consequently it is not a thermodynamic potential.

These remarks also concern other models in which similar ingredients and spectral decomposition of $\mathbf{D}$ are used (for example CHABOCHE [12]).

This study models quasi-brittle behaviour without any spectral or strain decomposition, while keeping the possibility of describing the salient phenomena related to damage.

In particular, the following effects are being dealt with:

(i) Physically sound damage configurations (corresponding to those obtained with the model by HALM AND DRAGON [6]) for a compressive loading path are modelled employing the present approach.

(ii) Analysis of the anisotropy induced by a given configuration of damage (for example for a set of parallel microcracks) shows that evolutions of elastic properties (namely Young's modulus and Poisson's ratio) are in agreement with micromechanically obtained results.

(iii) Recovery of the elastic properties at microcracks closure, known as unilateral effect, is taken into account.

In addition, the formulation advanced ensures dissipation positivity as well as continuity and uniqueness of free energy.

To reach this objective, anisotropic damage definition is first reconsidered. Consequently, this paper abandons the unique tensorial damage variable and presents a discrete damage formulation (Sec. 2). Starting from this definition, the Helmholtz free energy is redefined in Sec. 3, according to the tensor functions representation theory (BOEHLER [13]). The evolution laws are treated in Sec. 4 while maintaining the concern to account for predominant experimental facts observed for this class of materials. The salient points concerning the model's pertinency mentioned above (realistic damage configurations, induced anisotropy, recovery of moduli following microcracks closure, non-negativity of dissipation and continuity of free energy) are analyzed, commented and quantified in Secs. 5 and 6.

2. Damage variables: a discrete approach

The formalism of the thermodynamics of irreversible processes with internal variables is used (Germain *et al.* [14]). Unlike the original model summarized in Sec. 1, a discrete definition for the damage internal variables is proposed below.

2.1. A discrete damage definition

The present approach consists in considering different fixed directional tensors $\mathbf{N}_i = \mathbf{n}_i \otimes \mathbf{n}_i$, where $\mathbf{n}_i \in \Re^3$ and represents the normal to the crack, and attempting to associate them to scalar internal variables ρ_i representing the evolving microcrack densities.

Consequently, p independent couples$(\rho_i, \mathbf{N}_i = \mathbf{n}_i \otimes \mathbf{n}_i)$, $i \in [1, p]$, replace the unique damage variable $\mathbf{D}$, where each orientation $\mathbf{n}_i$ is fixed in the material point (i.e. in the physical space of the material corresponding to the representative volume element). Each associated microcrack density ρ_i is considered as an internal variable.

The scalar density ρ_i is physically related to the extent S of decohesion surface and the unit normal vector $\mathbf{n}_i$ describes orientation of the i-th set of parallel crack-like defects. Introduction of these couples is motivated by micromechanical considerations (see Kachanov [15]) but in the present context the density ρ_i is reckoned as a macroscopic quantity.

Two sets are then put forward:

- second-order tensors $\mathbf{N}_i$ of cracks orientation, which are preliminary parameters of the study;
- internal variables ρ_i associated with each $\mathbf{N}_i$.

The main difference between this definition and the single tensor $\mathbf{D}$ lies, in addition to the multiplication of the variables (while keeping a finite set of $\mathbf{N}_i$, sufficient from the operational viewpoint), in the fixed damage directions. Indeed, the single variable $\mathbf{D}$ has three eigenvectors which evolve during loading; here, these directions are *fixed* a priori and only the internal variables ρ_i vary; note that no spectral decomposition is made; consequently, the previously mentioned drawbacks are avoided.

The next step concerns the definition of a 'sufficient' number and of the specific orientations embodied by $\mathbf{N}_i$.

2.2. Choice of $\mathbf{N}_i$

The choice of $\mathbf{N}_i$ is assumed to fulfil two objectives:

(i) any tensor of the type $\mathbf{n} \otimes \mathbf{n}$ is an additive combination of $\mathbf{N}_i$;

(ii) an isotropic damage configuration (classically modelled with a damage tensor proportional to identity) should be represented by the same density ρ_0 in each direction $\mathbf{N}_i$:

$$\sum_i \rho_0 \mathbf{N}_i \propto \rho_0 \mathbf{I}, \tag{2.1}$$

where $\mathbf{I}$ is the second-order identity tensor.

To fulfil the first point, the set of $\mathbf{N}_i$ should generate the set of tensors of the type $\mathbf{n} \otimes \mathbf{n}$. As this set is of rank 6, there must be at least 6 $\mathbf{N}_i$. The canonical basis of the set $\mathbf{n} \otimes \mathbf{n}$ is the following:

$$\begin{aligned}
&\mathbf{N}_1 = \mathbf{e}_1 \otimes \mathbf{e}_1, \qquad \mathbf{N}_2 = \mathbf{e}_2 \otimes \mathbf{e}_2, \qquad \mathbf{N}_3 = \mathbf{e}_3 \otimes \mathbf{e}_3,\\
&\mathbf{N}_4 = \frac{1}{2}(\mathbf{e}_1 + \mathbf{e}_2) \otimes (\mathbf{e}_1 + \mathbf{e}_2), \qquad \mathbf{N}_5 = \frac{1}{2}(\mathbf{e}_1 + \mathbf{e}_3) \otimes (\mathbf{e}_1 + \mathbf{e}_3),\\
&\mathbf{N}_6 = \frac{1}{2}(\mathbf{e}_2 + \mathbf{e}_3) \otimes (\mathbf{e}_2 + \mathbf{e}_3),
\end{aligned} \tag{2.2}$$

where the triplet $(\mathbf{e}_1, \mathbf{e}_2, \mathbf{e}_3)$ forms an orthonormal basis of the Euclidean space $\Re^3$.

However, the sum of these tensors is not proportional to identity:

$$\sum_{i=1}^{6} \rho_0 \mathbf{N}_i \propto \rho_0 \begin{bmatrix} 2 & 1 & 1 \\ 1 & 2 & 1 \\ 1 & 1 & 2 \end{bmatrix}. \tag{2.3}$$

Three tensors are consequently added to fulfil relation (2.1):

$$\begin{aligned}
\mathbf{N}_7 &= \frac{1}{2}(\mathbf{e}_1 - \mathbf{e}_2) \otimes (\mathbf{e}_1 - \mathbf{e}_2),\\
\mathbf{N}_8 &= \frac{1}{2}(\mathbf{e}_1 - \mathbf{e}_3) \otimes (\mathbf{e}_1 - \mathbf{e}_3)\\
\mathbf{N}_9 &= \frac{1}{2}(\mathbf{e}_2 - \mathbf{e}_3) \otimes (\mathbf{e}_2 - \mathbf{e}_3).
\end{aligned} \tag{2.4}$$

The corresponding set of nine $\mathbf{N_i}$ tensors meets the above requirements:

$$
\begin{aligned}
&\mathbf{N}_1 = \mathbf{e}_1 \otimes \mathbf{e}_1, \qquad \mathbf{N}_2 = \mathbf{e}_2 \otimes \mathbf{e}_2, \qquad \mathbf{N}_3 = \mathbf{e}_3 \otimes \mathbf{e}_3,\\
&\mathbf{N}_4 = \frac{1}{2}(\mathbf{e}_1 + \mathbf{e}_2) \otimes (\mathbf{e}_1 + \mathbf{e}_2), \qquad \mathbf{N}_5 = \frac{1}{2}(\mathbf{e}_1 + \mathbf{e}_3) \otimes (\mathbf{e}_1 + \mathbf{e}_3),\\
&\mathbf{N}_6 = \frac{1}{2}(\mathbf{e}_2 + \mathbf{e}_3) \otimes (\mathbf{e}_2 + \mathbf{e}_3), \qquad \mathbf{N}_7 = \frac{1}{2}(\mathbf{e}_1 - \mathbf{e}_2) \otimes (\mathbf{e}_1 - \mathbf{e}_2),\\
&\mathbf{N}_8 = \frac{1}{2}(\mathbf{e}_1 - \mathbf{e}_3) \otimes (\mathbf{e}_1 - \mathbf{e}_3), \qquad \mathbf{N}_9 = \frac{1}{2}(\mathbf{e}_2 - \mathbf{e}_3) \otimes (\mathbf{e}_2 - \mathbf{e}_3).
\end{aligned}
\tag{2.5}
$$

Figure 1 shows, in the $(\mathbf{e}_1, \mathbf{e}_2)$ plane, the corresponding directions $\mathbf{n}_i$; the representation is the same in all $(\mathbf{e}_i, \mathbf{e}_j)$ planes $\left((i,j) \in [1,3]^2, i \neq j\right)$:

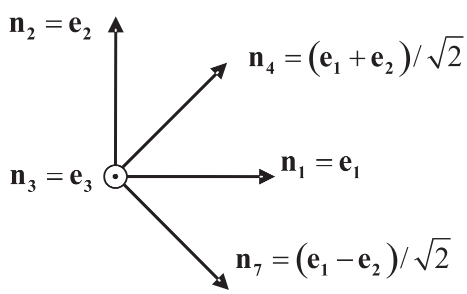

FIG. 1. Cracks directions in the $(\mathbf{e}_1, \mathbf{e}_2)$plane.

The choice of the space basis $(\mathbf{e}_1, \mathbf{e}_2, \mathbf{e}_3)$ is explained in Sec. 4.4.

Consequently, this system of nine fixed symmetric second-order tensors, representing nine microcracks directions, associated to nine densities as internal variables, is selected to enter the thermodynamic potential. It will play the same role as the tensorial variable $\mathbf{D}$, namely it will affect the elastic properties of the material.

REMARK 1. As shown in Sec. 4, microcracks growth can be non self-similar, since their orientation can change due to complex loading path. The approach presented, employing nine fixed directions, accounts approximately for this experimental fact.

3. Thermodynamic potential and constitutive laws

The framework of irreversible processes in thermodynamics with internal variables is here developed using the discrete approach of damage described in Sec. 2.

3.1. Thermodynamic potential without unilateral effect

The Helmholtz free energy w per unit volume is chosen as thermodynamic potential.

At this stage of model formulation, the following assumptions are made:

(i) the undamaged material is considered as isotropic,

(ii) the strain-stress response is supposed to be linear at constant damage: w is at most quadratic in $\boldsymbol{\varepsilon}$,

(iii) microcrack lips are assumed to slide without friction,

(iv) the effects of residual stresses are neglected: w does not contain any term linear in $\boldsymbol{\varepsilon}$ and linear in ρ_i (contrarily to Halm and Dragon [6]),

(v) microcracks densities are assumed to be moderate: w is consequently linear in ρ_i,

(vi) the nine microcracks systems do not interact: w is an additive form of elementary energies corresponding to one system of microcracks,

(vii) the influence of microcracks is only due to their orientation and densities (to $\mathbf{N}_i$ and ρ_i): material parameters are identical for all cracks.

According to the tensor functions representation theory (Boehler [13]), considering the hypotheses introduced in the foregoing and recalling $\|\mathbf{n}_i\| = 1$, the following expression is obtained for w:

$$w(\boldsymbol{\varepsilon}, \rho_i) = \frac{\lambda}{2}\operatorname{tr}^2(\boldsymbol{\varepsilon}) + \mu\operatorname{tr}(\boldsymbol{\varepsilon}.\boldsymbol{\varepsilon}) + \sum_{i=1}^{9}\rho_i\left\{C_1\operatorname{tr}^2(\boldsymbol{\varepsilon}) + C_2\operatorname{tr}(\boldsymbol{\varepsilon}.\boldsymbol{\varepsilon}) + \alpha\operatorname{tr}(\boldsymbol{\varepsilon})\operatorname{tr}(\boldsymbol{\varepsilon}.\mathbf{N}_i) + 2\beta\operatorname{tr}(\boldsymbol{\varepsilon}.\boldsymbol{\varepsilon}.\mathbf{N}_i) + \gamma\operatorname{tr}^2(\boldsymbol{\varepsilon}.\mathbf{N}_i)\right\} \tag{3.1}$$

where λ, μ are Lamé coefficients and $C_1, C_2, \alpha, \beta, \gamma$ are material parameters to be identified.

3.2. Unilateral effect

In the previous paragraph the unilateral effect is not taken into account. To represent correctly this important effect in the behaviour of quasi-brittle materials, it is necessary:

(i) to ensure the continuity and derivability of the free energy at opening/closure: even if the stiffness matrix $\mathbf{C} = \dfrac{\partial^2 w}{\partial\boldsymbol{\varepsilon}\partial\boldsymbol{\varepsilon}}$ (representing elastic properties) is discontinuous when passing from open to closed microcracks (and inversely), both free energy and stress strain response should remain continuous,

(ii) to find an opening/closure condition for each system of microcracks,

(iii) to define the recovery conditions, i.e. which elastic properties are restored when passing from an open state to a closed one.

3.2.1. Derivability at closure. Two states can be considered for w (and the deduced stiffness matrix), namely an open and a closed one; each material constant can consequently have an open and a closed value:

$$\begin{aligned}
w_{\text{open}}(\boldsymbol{\varepsilon},\rho_i;\mathbf{N}_i) &= w_0(\boldsymbol{\varepsilon}) + \sum_{i=1}^{9}\rho_i\Big\{C_1^{\text{open}}\operatorname{tr}^2(\boldsymbol{\varepsilon}) + C_2^{\text{open}}\operatorname{tr}(\boldsymbol{\varepsilon}.\boldsymbol{\varepsilon}) \\
&\quad + \alpha^{\text{open}}\operatorname{tr}(\boldsymbol{\varepsilon})\operatorname{tr}(\boldsymbol{\varepsilon}.\mathbf{N}_i) + 2\beta^{\text{open}}\operatorname{tr}(\boldsymbol{\varepsilon}.\boldsymbol{\varepsilon}.\mathbf{N}_i) + \gamma^{\text{open}}\operatorname{tr}^2(\boldsymbol{\varepsilon}.\mathbf{N}_i)\Big\}, \\
w_{\text{closed}}(\boldsymbol{\varepsilon},\rho_i;\mathbf{N}_i) &= w_0(\boldsymbol{\varepsilon}) + \sum_{i=1}^{9}\rho_i\Big\{C_1^{\text{closed}}\operatorname{tr}^2(\boldsymbol{\varepsilon}) + C_2^{\text{closed}}\operatorname{tr}(\boldsymbol{\varepsilon}.\boldsymbol{\varepsilon}) \\
&\quad + \alpha^{\text{closed}}\operatorname{tr}(\boldsymbol{\varepsilon})\operatorname{tr}(\boldsymbol{\varepsilon}.\mathbf{N}_i) + 2\beta^{\text{closed}}\operatorname{tr}(\boldsymbol{\varepsilon}.\boldsymbol{\varepsilon}.\mathbf{N}_i) + \gamma^{\text{closed}}\operatorname{tr}^2(\boldsymbol{\varepsilon}.\mathbf{N}_i)\Big\},
\end{aligned} \tag{3.2}$$

where $w_0(\boldsymbol{\varepsilon}) = \dfrac{\lambda}{2}\operatorname{tr}^2(\boldsymbol{\varepsilon}) + \mu\operatorname{tr}(\boldsymbol{\varepsilon}.\boldsymbol{\varepsilon})$ is the classic Hooke's law.

It is then possible to define the elementary energy w_i corresponding to one system of microcracks:

$$\begin{aligned}
w_{\text{open}}(\boldsymbol{\varepsilon},\rho_i;\mathbf{N}_i) &= w_0(\boldsymbol{\varepsilon}) + \sum_{i=1}^{9} w_i^{\text{open}}(\boldsymbol{\varepsilon},\rho_i;\mathbf{N}_i), \\
w_{\text{closed}}(\boldsymbol{\varepsilon},\rho_i;\mathbf{N}_i) &= w_0(\boldsymbol{\varepsilon}) + \sum_{i=1}^{9} w_i^{\text{closed}}(\boldsymbol{\varepsilon},\rho_i;\mathbf{N}_i).
\end{aligned} \tag{3.3}$$

Calling $k_i(\boldsymbol{\varepsilon})$ the scalar function separating the closed ($k_i(\boldsymbol{\varepsilon}) \le 0$) and open ($k_i(\boldsymbol{\varepsilon}) > 0$) domains for each microcracks system under the assumption $k_i(\mathbf{0}) = 0$, the elementary energy can take the following form:

$$w_i(\boldsymbol{\varepsilon},\rho_i;\mathbf{N}_i) = \begin{cases} w_i^{\text{open}}(\boldsymbol{\varepsilon},\rho_i;\mathbf{N}_i), & \text{if} \quad k(\boldsymbol{\varepsilon}) > 0 \\ w_i^{\text{closed}}(\boldsymbol{\varepsilon},\rho_i;\mathbf{N}_i), & \text{if} \quad k(\boldsymbol{\varepsilon}) \le 0. \end{cases} \tag{3.4}$$

Using Eq. (3.3):

$$w(\boldsymbol{\varepsilon},\rho_i;\mathbf{N}_i) = w_0(\boldsymbol{\varepsilon}) + \sum_{i=1}^{9} w_i(\boldsymbol{\varepsilon},\rho_i;\mathbf{N}_i). \tag{3.5}$$

To ensure the continuity of w, each w_i must fulfil the continuity requirements imposed by the multilinear functions theory (CURNIER *et al.* [16]): the stiffness discontinuity at closure $[\mathbf{C}_i] = \mathbf{C}_i^{\text{open}} - \mathbf{C}_i^{\text{closed}} = \dfrac{\partial^2\left(w_i^{\text{open}}(\boldsymbol{\varepsilon},\rho_i) - w_i^{\text{closed}}(\boldsymbol{\varepsilon},\rho_i)\right)}{\partial\boldsymbol{\varepsilon}.\partial\boldsymbol{\varepsilon}}$, corresponding to a system of parallel microcracks (normal to $\mathbf{n}_i$), must be nil (i.e. no rigidity recovery) or of rank 1; this latter condition gives some relations between material constants.

From Eqs. (3.2) and (3.5), $[\mathbf{C}]_i$ can be written in the following form in orthonormal basis $(\mathbf{n}_i, \mathbf{t}, \mathbf{k})$ of the Euclidean space $\Re^3$ (Voigt notation):

$$[\mathbf{C_i}] = \rho_i \begin{bmatrix} 2([\alpha]+2[\beta]+[C_1]+[C_2]+[\gamma]) & [\alpha]+2[C_1] & [\alpha]+2[C_1] & 0 & 0 & 0 \\ [\alpha]+2[C_1] & 2([C_1]+[C_2]) & 2[C_1] & 0 & 0 & 0 \\ [\alpha]+2[C_1] & 2[C_1] & 2([C_1]+[C_2]) & 0 & 0 & 0 \\ 0 & 0 & 0 & [C_2] & 0 & 0 \\ 0 & 0 & 0 & 0 & [C_2]+[\beta] & 0 \\ 0 & 0 & 0 & 0 & 0 & [C_2]+[\beta] \end{bmatrix} \tag{3.6}$$

where $[A] = A^{\text{open}} - A^{\text{closed}}$.

Micromechanical studies (KACHANOV [15]) provide the expression of the compliance of a material containing non-interacting penny-shaped microcracks. These results underscore that the quadratic terms in $\mathbf{N}_i$ (i.e. $\mathbf{N}_i \otimes \mathbf{N}_i$) entering the compliance when microcracks are open is negligible compared to the other terms. Here, the only term of $\mathbf{C}_i^{\text{open}}$ in which intervenes the dyadic product $\mathbf{N}_i \otimes \mathbf{N}_i$ is $2\,\gamma^{\text{open}}\,\mathbf{N}_i \otimes \mathbf{N}_i$. Consequently, the parameter γ^{open} is taken equal to zero and $[\gamma] = -\gamma^{\text{closed}} = -\gamma$.

It results that the following relations are sufficient to ensure the continuity of w_i:

$$\begin{aligned} \alpha^{\text{open}} &= \alpha^{\text{closed}} = \alpha, \\ \beta^{\text{open}} &= \beta^{\text{closed}} = \beta, \\ C_1^{\text{open}} &= C_1^{\text{closed}} = C_1, \\ C_2^{\text{open}} &= C_2^{\text{closed}} = C_2, \end{aligned} \tag{3.7}$$

The particular choice (3.7) is exempted from identifying parameters in the closed configuration since "closed" parameters are the same as "open" ones.

Only one term differs: unlike γ^{open}, γ^{closed} cannot be taken equal to zero, insofar the quadratic term $\mathbf{N}_i \otimes \mathbf{N}_i$ is no longer negligible when the cracks close.

At this stage, from Eqs. (3.6) and (3.7), $[\mathbf{C}_i]$ can be simplified:

$$[\mathbf{C}_i] = -2\gamma^{\text{closed}}\rho_i\, \mathbf{N}_i \otimes \mathbf{N}_i. \tag{3.8}$$

Curnier *et al.* ([16]) show that the continuous differentiability of w_i defined by (3.4) necessitates $[\mathbf{C}_i]$ to take the following form: $[\mathbf{C}_i] = s(\boldsymbol{\varepsilon}).\nabla k_i \otimes \nabla k_i$; this leads to the closure condition:

$$k_i(\boldsymbol{\varepsilon}) = (\mathbf{n}_i \otimes \mathbf{n}_i) : \boldsymbol{\varepsilon} = \mathbf{N}_i : \boldsymbol{\varepsilon} \leq 0 \tag{3.9}$$

The closure condition obtained here seems to be reasonable: cracks close when the normal strain $\operatorname{tr}(\boldsymbol{\varepsilon}.\mathbf{N}_i)$ becomes negative.

This reasoning is independent of the chosen $\mathbf{N}_i \leq 0$.

In view of relations (3.2), (3.7) and (3.9), the final form for w is the following:

$$\begin{aligned} w\,(\boldsymbol{\varepsilon}, \rho_i; \mathbf{N}_i) = w_0(\boldsymbol{\varepsilon}) + \sum_{i=1}^{9} \rho_i \left\{C_1 \operatorname{tr}^2(\boldsymbol{\varepsilon}) + C_2 \operatorname{tr}(\boldsymbol{\varepsilon}.\boldsymbol{\varepsilon}) \right. \\ \left. + \, \alpha \operatorname{tr}(\boldsymbol{\varepsilon})\, \operatorname{tr}(\boldsymbol{\varepsilon}.\mathbf{N_i}) + 2\beta \operatorname{tr}(\boldsymbol{\varepsilon}.\boldsymbol{\varepsilon}.\mathbf{N}_{\mathrm{i}}) + \gamma \operatorname{tr}^2(\boldsymbol{\varepsilon}.\mathbf{N}_i)\,.H(-\operatorname{tr}(\boldsymbol{\varepsilon}.\mathbf{N}_i))\right\}. \end{aligned} \tag{3.10}$$

The free energy determined with the continuity conditions still contains five different parameters to identify $(C_1, C_2, \alpha, \beta, \gamma)$, in addition to the classic Lamé coefficients. However, recovery conditions permit to find relations between these coefficients (see Halm and Dragon [6]).

3.2.2. Recovery conditions. Since microcracks are assumed not to interact, only one system of parallel microcracks normal to $\mathbf{n}_i$ is studied (other densities are taken equal to zero). It is assumed that the normal Young's modulus, denoted $E(\mathbf{n}_i)$, is restored to its initial value E_0 when cracks close (i.e. when $\operatorname{tr}(\boldsymbol{\varepsilon}.\mathbf{N}_i) \leq 0$).

This assumption is written considering an uniaxial compression loading path in the direction normal to the cracks ($\boldsymbol{\sigma} = \sigma\, \mathbf{n}_i \otimes \mathbf{n}_i$).

Using definition (3.10), the restoration of normal Young's modulus leads to three scalar relations, allowing to express C_1, C_2 and γ as functions of α and β:

$$\left\{\begin{aligned} C_1 + C_2 + \alpha + 2\beta + \gamma = 0 \\ 2\,C_1 + \alpha = 0 \\ 2\,C_1 + C_2 = 0 \end{aligned}\right. \quad \Leftrightarrow \quad \left\{\begin{aligned} & C_1 = -\frac{\alpha}{2} \\ & C_2 = \alpha. \\ & \gamma = -\left(\frac{3}{2}\alpha + 2\,\beta\right) \end{aligned}\right. \tag{3.11}$$

Conjugating relations (3.11) and expression (3.10), the final Helmholtz free energy is obtained as follows:

$$
\begin{aligned}
(3.12) \qquad w\left(\boldsymbol{\varepsilon},\rho_i;\mathbf{N}_i\right) = w_0(\boldsymbol{\varepsilon}) + \sum_{i=1}^{9}\rho_i \Bigg\{ \alpha \left[\operatorname{tr}\left(\boldsymbol{\varepsilon}.\boldsymbol{\varepsilon}\right) - \frac{1}{2}\operatorname{tr}^2\left(\boldsymbol{\varepsilon}\right) + \operatorname{tr}\left(\boldsymbol{\varepsilon}\right)\operatorname{tr}\left(\boldsymbol{\varepsilon}.\mathbf{N}_i\right)\right] \\
+ 2\,\beta\operatorname{tr}\left(\boldsymbol{\varepsilon}.\boldsymbol{\varepsilon}.\mathbf{N}_i\right) - \left(\frac{3}{2}\alpha + 2\,\beta\right)\operatorname{tr}^2\left(\boldsymbol{\varepsilon}.\mathbf{N}_i\right).H(-\operatorname{tr}(\boldsymbol{\varepsilon}.N_i))\Bigg\}.
\end{aligned}
$$

REMARK 2. Other recovery conditions may be chosen:

- Restoration of the bulk modulus in all directions as experimentally observed by SIBAÏ *et al.* [17].
- Restoration of the elongation modulus normal to the crack has been shown by a micromechanical analysis (PENSÉE and KONDO [18]).

Relation (3.11) takes into account each of these restoration conditions. Their combination would lead exactly to relation (3.11).

Finally, relation (3.11) ensures restoration of any $\boldsymbol{\nu}_{n_i,\mathbf{t}}$, (where $\mathbf{t}$ is orthogonal to $\mathbf{n}_i$) Poisson's ratio.

From the thermodynamic potential (3.12), the constitutive laws ('state laws') can be determined.

3.3. State laws

The state laws define the strain-stress relation and the thermodynamic forces associated with the internal variables. They are obtained by differentiating the potential (3.12).

Consequently, the strain-stress relation is the following:

$$
\begin{aligned}
(3.13) \qquad \boldsymbol{\sigma}(\boldsymbol{\varepsilon},\rho_i;\mathbf{N}_i) &= \frac{\partial w(\boldsymbol{\varepsilon},\rho_i;\mathbf{N}_i)}{\partial\boldsymbol{\varepsilon}} \\
&= \lambda\operatorname{tr}(\boldsymbol{\varepsilon})\,\mathbf{I} + 2\mu\,\boldsymbol{\varepsilon} + \sum_{i=1}^{9}\rho_i\Big\{\alpha\left[2\,\boldsymbol{\varepsilon} - \operatorname{tr}(\boldsymbol{\varepsilon})\,\mathbf{I} + \operatorname{tr}(\boldsymbol{\varepsilon})\,\mathbf{N}_i + \operatorname{tr}(\boldsymbol{\varepsilon}.\mathbf{N}_i)\mathbf{I}\right] \\
&\quad + 2\,\beta\left[\boldsymbol{\varepsilon}.\mathbf{N}_i + \mathbf{N}_i.\boldsymbol{\varepsilon}\right] - (3\,\alpha + 4\,\beta)\operatorname{tr}(\boldsymbol{\varepsilon}.\mathbf{N}_i)H\left(-\operatorname{tr}(\boldsymbol{\varepsilon}.\mathbf{N}_i)\right)\mathbf{N}_i\Big\}.
\end{aligned}
$$

The nine thermodynamic forces corresponding to each density variable are derived from w as follows:

$$
\begin{aligned}
(3.14) \qquad F^{\rho_i}\left(\boldsymbol{\varepsilon}_i;\mathbf{N}_i\right) &= -\frac{\partial w(\boldsymbol{\varepsilon},\rho_i;\mathbf{N}_i)}{\partial\rho_i} \\
&= -\alpha\left[\operatorname{tr}\left(\boldsymbol{\varepsilon}.\boldsymbol{\varepsilon}\right) - \frac{1}{2}\operatorname{tr}^2(\boldsymbol{\varepsilon}) + \operatorname{tr}\left(\boldsymbol{\varepsilon}\right)\,\operatorname{tr}\left(\boldsymbol{\varepsilon}.\mathbf{N}_i\right)\right] - 2\beta\operatorname{tr}\left(\boldsymbol{\varepsilon}.\boldsymbol{\varepsilon}.\mathbf{N_i}\right) \\
&\quad + \left(\frac{3}{2}\alpha + 2\beta\right)\operatorname{tr}^2\left(\boldsymbol{\varepsilon}.\mathbf{N}_i\right)H\left(-\operatorname{tr}\left(\boldsymbol{\varepsilon}.\mathbf{N}_i\right)\right).
\end{aligned}
$$

In this paragraph, the elastic response (3.13) of a quasi-brittle material has been defined under different assumptions for a given fixed state of damage (represented by different ρ_i).

To complete this model, the evolution laws for these damage variables need to be constructed.

4. Reversibility domain and evolution laws

The purpose of this section is to determine *when* and *how* the damage, represented by the internal variables ρ_i and directional, fixed parameters $\mathbf{N}_i$, evolve.

4.1. Experimental facts

As mentioned in the introduction, the initial nucleation and subsequent growth of the microcracks in quasi-brittle materials is a complex phenomenon which leads to an induced anisotropy. In order to model properly the behaviour of these materials, it is essential that the modelled damage process should fit the physical observations. A synthesis of these observations can be found for example in Fanella and Krajcinovic [1], Horii and Nemat-Nasser [19] and Ju [20], and other studies.

For concrete subjected to uniaxial compression, it has been observed that microcracks first grow in a Mode II fashion (remaining closed) along the aggregate facet (Fig. 2a and b). This growth is unstable. However, it is stopped at the

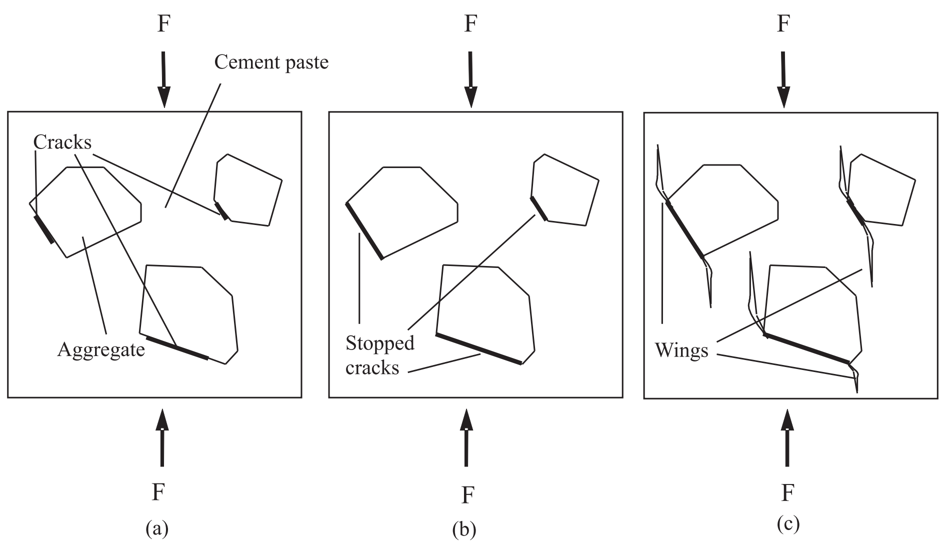

Fig. 2. Crack growth phases under compression: a) Initial state, b) Mode II growth, c) Kinking of the crack in the cement paste.

edge of the aggregate facet (since the toughness of the cement paste is greater than the interface's one); consequently its length remains small (about the size of the aggregate). As the axial compression increases, the crack does not continue to grow in a Mode II fashion but develops tension wings at both tips. It then grows from the tips and curves toward the direction of maximum compression (Fig. 2c), and, consequently, the strain normal to the wings is positive (although it remains negative along the aggregate facet).

In a mesoscopic view, this microcrack can be split into a closed part (at the interface) whose length is fixed and into an open part, oriented in the direction of maximal compression, that keeps growing in the cement paste. As a conclusion, Mode II growth is not preponderant, even if it is the first one activated.

The resulting damage configuration seems to be a set of quasi-parallel microcracks oriented in the direction of maximum compression.

Under uniaxial tensile loads, microcracks grow in a Mode I fashion. Microcracks that are oriented perpendicularly to the load axis open and grow prior to the others. Note that not only perpendicular microcracks come to grow under tension; other open ones can grow. They nevertheless evolve remaining open. The resulting damage configuration (in a mesoscopic view) is then a set of open microcracks whose orientation is predominantly (but not exclusively) perpendicular to the maximum tensile direction. However, the density of the non-perpendicular cracks is lower; indeed, some reorientation (kink) in the perpendicular direction limits their growth. The final failure is consequently perpendicular to the tensile load axis.

From the different observations quoted before, cracks appear to grow principally when they are open.

4.2. Reversibility domains

The existence of a reversibility domain for each direction $\mathbf{N}_i$ (and the associated variables ρ_i) is assumed; it is written in the generalized space of the associated thermodynamic forces for time-independent evolution assumed further.

To take into account the experimental facts explained in Sec. 4.1, the thermodynamic forces (3.14) are split into two parts (relation (4.1)).

$$F^{\rho_i}(\boldsymbol{\varepsilon};\mathbf{N}_i) = -\frac{\partial w(\boldsymbol{\varepsilon},\rho_i;\mathbf{N}_i)}{\partial \rho_i} = \underbrace{-\alpha\left[\operatorname{tr}(\boldsymbol{\varepsilon}.\boldsymbol{\varepsilon}) - \frac{1}{2}\operatorname{tr}^2(\boldsymbol{\varepsilon}) + \operatorname{tr}(\boldsymbol{\varepsilon})\operatorname{tr}(\boldsymbol{\varepsilon}.\mathbf{N}_i)\right]}_{F_1^{\rho_i}(\boldsymbol{\varepsilon};\mathbf{N}_i)} \tag{4.1}$$

$$
\underbrace{-2\beta \operatorname{tr}\left(\boldsymbol{\varepsilon}.\boldsymbol{\varepsilon}.\mathbf{N}_i\right) + \left(\frac{3}{2}\alpha + 2\beta\right) \operatorname{tr}^2\left(\boldsymbol{\varepsilon}.\mathbf{N}_i\right)}_{F_1^{\rho_i}\left(\boldsymbol{\varepsilon};\mathbf{N}_i\right)}
\tag{4.1 [cont.]}
$$

$$
\underbrace{-\left(\frac{3}{2}\alpha + 2\beta\right) \operatorname{tr}^2\left(\boldsymbol{\varepsilon}.\mathbf{N}_i\right) + \left(\frac{3}{2}\alpha + 2\beta\right) \operatorname{tr}^2\left(\boldsymbol{\varepsilon}.\mathbf{N}_i\right) H\left(-\operatorname{tr}\left(\boldsymbol{\varepsilon}.\mathbf{N}_i\right)\right)}_{F_2^{\rho_i}\left(\boldsymbol{\varepsilon};\mathbf{N}_i\right)}.
$$

This decomposition permits to distinguish two parts in the global F^{ρ_i}:

(i) the first term, $F_1^{\rho_i}$, that contains both non-directional terms (see terms $\operatorname{tr}(\boldsymbol{\varepsilon}.\boldsymbol{\varepsilon})$ and $\operatorname{tr}^2(\boldsymbol{\varepsilon})$ in which direction $\mathbf{N}_i$ does not intervene) and the oriented ones; as this term can reach a positive value (and consequently the elastic limit) even if cracks are closed, it will not enter the reversibility domain;

(ii) a normal part, $F_2^{\rho_i}$, that depends only on the normal strain $\operatorname{tr}(\boldsymbol{\varepsilon}.\mathbf{N}_i)$ and reduces to zero when cracks are closed ($\operatorname{tr}(\boldsymbol{\varepsilon}.\mathbf{N}_i) \leq 0$); this part is the one that will limit the elastic domain, since the experimental considerations show that microcracks evolve only when they are open.

The following form for any reversibility domain is postulated:

$$
f_i(F_2^{\rho_i}, \rho_i) = F_2^{\rho_i} - C_0\, e^{\rho_i/C_3} \leq 0, \qquad i \in [1, 9]\,, \tag{4.2}
$$

where C_0 is a material constant that represents the initial limit of the elastic domain, and C_3 influences the microcrack growth: the higher this constant is, the higher the densities will be.

Since the material is assumed to be initially isotropic, cracks can grow a priori in all directions in an equivalent way; only the loading path, contained in the thermodynamic forces, will determine which system will be activated: the same C_0 and C_3 are used for all directions $\mathbf{N}_i$.

Remark 3. According to experimental considerations, microcracks can grow in a non self-similar way and kink towards the direction of maximum compression. This orientation change can also occur due to complex loading. In the present discrete approach, the nine directions are fixed. However, when the loading directions change, as $F_2^{\rho_i}$ depends on the current strain, the evolution of ρ_i will follow; densities ρ_i increase only if its associated driving force $F_2^{\rho_i}$ reaches the elastic limit $C_0\, e^{\rho_i/C_3}$ moreover, the higher $F_2^{\rho_i}$ is (i.e. the higher $\operatorname{tr}(\boldsymbol{\varepsilon}.\mathbf{N}_i)$ is), the more ρ_i increases (see expression (4.5) further). In the case shown in Fig. 3, the 'real' crack evolution (Fig. 3a) is split into 2 parts (Fig. 3b). During the first stage, its growth, self-similar, would be taken into account in the model by the evolution of ρ_2 (as $\mathbf{n}_2$ corresponds to its normal $\mathbf{n}$); during the second stage, as the wing normal turns to $\mathbf{n}'$ which is parallel to $\mathbf{n}_7$, ρ_7 will evolve. This change of evolving density accounts for the microcrack direction change.

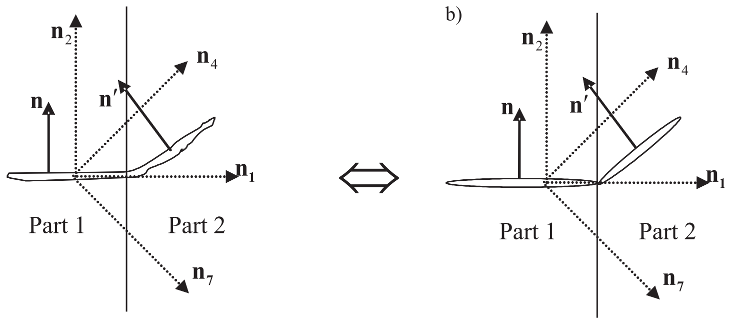

Fig. 3. Changing crack direction case: a) real crack; b) corresponding cracks in the model.

4.3. Evolution laws

In the present case, within the assumption of a time-independent process, a *non-associated* framework is used.

In an *associated* framework, the existence of a dissipation potential Φ depending on the damage flow variables (the set $(\dot{\rho}_i,\ i \in [1,9])$) is assumed; its Legendre–Fenchel transform defines a dissipation pseudo-potential $\Phi^*(F^{\rho_i},\ i \in [1,9])$, dual of Φ regarding the flow variables $(\dot{\rho}_i,\ i \in [1,9])$. This pseudo-potential Φ^* is the indicator function of the convex $\mathcal{C}$ of admissible thermodynamic forces $F^{\rho_i}, i \in [1,9]$ (the reversibility domain), that is consequently built upon the thermodynamic forces, that is to say dependent on *complete* thermodynamic forces F^{ρ_i}, $i \in [1,9]$. The damage evolution is normal to $\mathcal{C}$ (i.e. $\dot{\rho}_i \in \partial_{F^{\rho_i}}\Phi^*,\ i \in [1,9]$), where $\partial_{F^{\rho_i}}\Phi^*$ is the subdifferential of Φ^* at point F^{ρ_i}.

In the present case, the evolution of damage variables $(\rho_i,\ i \in [1,9])$ is defined independently of the reversibility domains (4.2). These domains, indicating *"when"* the damage evolves, depend only on the normal parts $F_2^{\rho_i}$ of thermodynamic forces. The damage evolution (indicating *"how"* the damage evolves) is on the contrary established in the space of complete driving (thermodynamic) forces with the functions $F_i\left(F^{\rho_i}\right)$ as follows:

$$F_i\left(F^{\rho_i}\right) = F^{\rho_i}, \qquad i \in [1,9]\,. \tag{4.3}$$

The evolution is thus defined as based on the potentials $F_i\left(F^{\rho_i}\right)$ relevant to each particular mechanism:

$$\dot{\rho}_i = \dot{\Lambda}_i \frac{\partial F_i}{\partial F^{\rho_i}} = \dot{\Lambda}_i, \quad \dot{\Lambda}_i \geq 0, \quad f_i \leq 0, \quad \dot{\Lambda}_i . f_i = 0, \quad i \in [1,9] \tag{4.4}$$

where $\dot{\Lambda}_i$ are damage multipliers.

The consistency condition on elastic domains (4.2) gives the expression of these multipliers:

$$\dot{f}_i = 0 \Rightarrow \dot{\Lambda}_i = -\frac{C_3\ (3\alpha + 4\beta)\ \mathrm{tr}\,(\boldsymbol{\varepsilon}.\mathbf{N}_i)\ H\,[\mathrm{tr}\,(\boldsymbol{\varepsilon}.\mathbf{N}_i)]}{C_0\, e^{\rho_i/C_3}}\mathbf{N}_i : \dot{\boldsymbol{\varepsilon}}, \quad i \in [1, 9]\,. \tag{4.5}$$

Expression (4.5) shows that a microcrack density ρ_i can evolve only if the opening condition $\mathrm{tr}\,(\boldsymbol{\varepsilon}.\mathbf{N}_i) \geq 0$ is satisfied.

REMARK 4. The evolution laws presented above are not standard in the sense of HALPHEN and NGUYEN [21]:

(i) the convex domains of admissible thermodynamic forces (4.2) are based on a specific partition (physically motivated) of these forces instead of depending on the global ones F^{ρ_i};

(ii) the potentials $F_i\,(F^{\rho_i})$ relevant to the mechanisms at stake are equivalent to complete thermodynamic forces: the model is thus non-associated.

4.4. Choice of the space basis $(\mathbf{e}_1, \mathbf{e}_2, \mathbf{e}_3)$

As explained in Sec. 2.2, the definition of the 9 different directions $\mathbf{N}_i$ uses an orthonormal basis $(\mathbf{e}_1, \mathbf{e}_2, \mathbf{e}_3)$ of the physical space $\Re^3$. The choice of this basis is explained in this section.

In practice, this first vector $\mathbf{e}_1$ is defined as the first direction of damage activation. The objective is then to find the direction $\mathbf{n}$ in which the elastic limit is first reached, and to impose $\mathbf{e}_1 = \mathbf{n}$.

Expression (4.2) shows that this direction is the one that maximizes the thermodynamic force F_2^{ρ} over all directions. It can be geometrically found using expression (4.1) and Fig. 4 where $\boldsymbol{\varepsilon}_1$, $\boldsymbol{\varepsilon}_2$ and $\boldsymbol{\varepsilon}_3$ are the three eigenvalues of the strain tensor, with convention $\boldsymbol{\varepsilon}_1 \geq \boldsymbol{\varepsilon}_2 \geq \boldsymbol{\varepsilon}_3$. Indeed, remembering $\mathbf{N} = \mathbf{n} \otimes \mathbf{n}$, the active part F_2^{ρ} of thermodynamic force (4.1) can be written:

$$F_2^{\rho}(\boldsymbol{\varepsilon}; \mathbf{n}) = -\left(\frac{3}{2}\alpha + 2\beta\right)(\mathbf{n}.\boldsymbol{\varepsilon}.\mathbf{n}).(\mathbf{n}.\boldsymbol{\varepsilon}.\mathbf{n})H\,(\mathbf{n}.\boldsymbol{\varepsilon}.\mathbf{n})\,. \tag{4.6}$$

Expression (4.6) and Fig. 4 show that thermodynamic force F_2^{ρ} is represented in the open zone by the square of $\boldsymbol{\varepsilon}_{nn}$; in the closed one it reduces to zero.

The direction $\mathbf{e}_1$ maximizing the force consequently corresponds to the maximal positive eigenvalues of the strain tensor. In other words, the effect is analogous to the classically used strain partition and the positive part $\boldsymbol{\varepsilon}^+$ is obtained without resort to the corresponding projection operators.

Knowing the first direction $\mathbf{e}_1$, the two other directions are arbitrarily chosen to form an orthogonal direct basis. Indeed in the plane orthogonal to $\mathbf{e}_1$, Eqs. (2.2) indicate that four directions are considered, separated by 45° angle; consequently, the description appears sufficient whatever vectors $\mathbf{e}_2$ and $\mathbf{e}_3$ are.

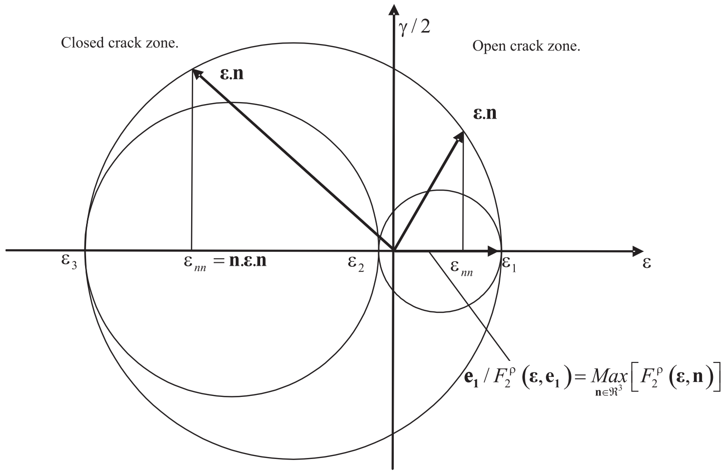

FIG. 4. Mohr circle allowing to find the optimal direction.

REMARK 5. Resulting from the definition of the nine crack directions and from the choice of the $(\mathbf{e}_1, \mathbf{e}_2, \mathbf{e}_3)$ basis described above, principal axes of the strain tensor (for the first loading path that reaches the elastic limit) are always included in the set of $\mathbf{N}_i$.

REMARK 6. In the case of 2 or 3 positive and equal eigenvalues, the vector $\mathbf{e}_1$ is arbitrarily taken in the eigenplane.

REMARK 7. As the $(\mathbf{e}_1, \mathbf{e}_2, \mathbf{e}_3)$ basis is chosen for the first loading path which reaches the elastic limit, the subsequent behaviour modelled will be conditioned by this first loading path. This corresponds to experimental observations: indeed, DEFLANDRE *et al.* [22] show, using an acoustic emission analysis on different quasi-brittle rocks, that the elastic stage is shorter than the linear phase of the stress-strain diagram, because crack creation occurs before the globally averaged elastic limit is attained for a representative volume. Consequently, the first damaging loading path would have consequences on further material behaviour, even if it just reaches the damage threshold. This justifies the fact that further crack directions are influenced by it.

5. Predictive capacities of the model

The predictive capacities of the model presented in the previous sections are now studied. The effective elastic properties at constant damage for a Vosges sandstone are first evaluated; simulations of a triaxial axisymmetric compression loading path are then shown for the same material.

5.1. Effective elastic properties at constant damage

In this part, a sample weakened by a set of parallel microcracks of normal $\mathbf{n}_1 = \mathbf{e}_1$ and density $\rho_1 = 0.15$ is considered. The induced elastic properties depend on this damage configuration: cracks can be open or closed.

In the open case, i.e. when $\boldsymbol{\varepsilon}_1 > 0$, the stiffness matrix expression is the following (Voigt notation):

$$\mathbf{C}_{\text{open}} = \begin{bmatrix} \lambda + 2\mu + \rho_1(3\alpha + 4\beta) & \lambda & \lambda & 0 & 0 & 0 \\ \lambda & \lambda + 2\mu + \rho_1\alpha & \lambda - \rho_1\alpha & 0 & 0 & 0 \\ \lambda & \lambda - \rho_1\alpha & \lambda + 2\mu + \rho_1\alpha & 0 & 0 & 0 \\ 0 & 0 & 0 & \mu + \rho_1\alpha & 0 & 0 \\ 0 & 0 & 0 & 0 & \mu + \rho_1(\alpha+\beta) & 0 \\ 0 & 0 & 0 & 0 & 0 & \mu + \rho_1(\alpha+\beta) \end{bmatrix}. \tag{5.1}$$

In the closed case ($\boldsymbol{\varepsilon}_1 < 0$), it takes the form:

$$\mathbf{C}_{\text{closed}} = \begin{bmatrix} \lambda + 2\mu & \lambda & \lambda & 0 & 0 & 0 \\ \lambda & \lambda + 2\mu + \rho_1\alpha & \lambda - \rho_1\alpha & 0 & 0 & 0 \\ \lambda & \lambda - \rho_1\alpha & \lambda + 2\mu + \rho_1\alpha & 0 & 0 & 0 \\ 0 & 0 & 0 & \mu + \rho_1\alpha & 0 & 0 \\ 0 & 0 & 0 & 0 & \mu + \rho_1(\alpha+\beta) & 0 \\ 0 & 0 & 0 & 0 & 0 & \mu + \rho_1(\alpha+\beta) \end{bmatrix}. \tag{5.2}$$

The definitions of the Young modulus $E(\mathbf{m})$ related to the direction of unit vector $\mathbf{m}$ and of the Poisson ratio $\nu(\mathbf{m}, \mathbf{p})$ related to orthogonal directions of respective unit vectors $\mathbf{m}$ and $\mathbf{p}$ can be derived from the stiffness tensor $\mathbf{C}$ (HAYES [23]):

$$
\begin{aligned}
E(\mathbf{m}) &= \left[\mathbf{m}\otimes\mathbf{m} : \mathbf{C}^{-1} : \mathbf{m}\otimes\mathbf{m}\right]^{-1},\\
\nu(\mathbf{m},\mathbf{p}) &= E(\mathbf{m})\left[\mathbf{m}\otimes\mathbf{m} : \mathbf{C}^{-1} : \mathbf{p}\otimes\mathbf{p}\right].
\end{aligned}
\tag{5.3}
$$

Figure 5 shows these two elastic properties for a Vosges sandstone weakened by this damage configuration. Vectors $\mathbf{m}$, $\mathbf{p}$, $\mathbf{e}_1$ and $\mathbf{e}_2$ are coplanar.

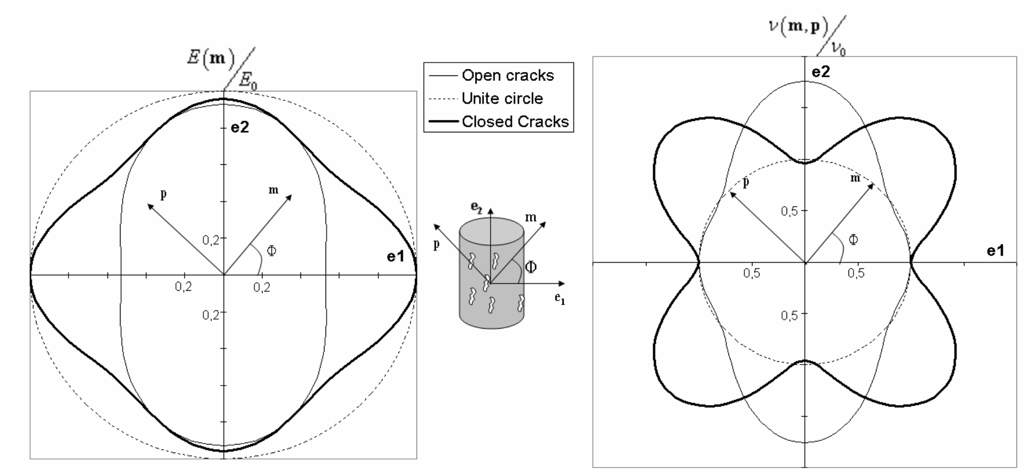

FIG. 5. Generalized elastic moduli normalized by their initial values.

The parameters (α, β, C_0 and C_3) taken for this analysis have been identified for a triaxial loading path with a 10 MPa confinement pressure (PECQUEUR [24]). For this material, these parameters take the following values:

$$
\begin{aligned}
\lambda &= 3245\,\mathrm{MPa},\\
\mu &= 5340\,\mathrm{MPa},\\
\alpha &= -2500\,\mathrm{MPa},\\
\beta &= -8100\,\mathrm{MPa},\\
C_0 &= 4.22\times\,10^{-3}\,\mathrm{MPa},\\
C_3 &= 2.33\times 10^{-2}.
\end{aligned}
\tag{5.4}
$$

In the open case, $E(\mathbf{m})$ and $\nu(\mathbf{m},\mathbf{p})$ are both degraded anisotropically, with a main degradation in the direction normal to the crack (namely $E(\mathbf{e}_1)$ and

$\nu(\mathbf{e}_2, \mathbf{e}_1)$). The slight Young's modulus degradation in the crack plane (here $E(\mathbf{e}_2)$) is due to the "isotropic" terms $\mathrm{tr}\,(\boldsymbol{\varepsilon}.\boldsymbol{\varepsilon})$ and $\mathrm{tr}^2\,(\boldsymbol{\varepsilon})$ in the free energy; this degradation is, in this particular case, 1.8 times lower than in the normal direction. The Poisson ratio $\nu(\mathbf{e}_2, \mathbf{e}_1)$ increases when the material is weakened; if no experimental results can validate or invalidate this remark, it can be noted that some models lead to increase (DRAGON and HALM [7] for example) and others to decrease (KACHANOV [25]) this Poisson ratio. In our case, $\nu\,(\mathbf{e_1}, \mathbf{e_2})$ is not degraded for both configurations (open and closed microcracks). Indeed its expression is the same whenever cracks are open or closed; its recovery at closure implies that it remains equal to its initial value, even if the material is weakened.

When microcracks are closed, the restoration of Young's modulus and Poisson's ratio depends on the considered direction: in the normal one, both of them are equal to their initial values, in accordance with the recovery conditions assumed in Sec. 3. In other directions, the recovery is partial; the Young's modulus in the crack plane $E\,(\mathbf{e}_2)$ remains degraded, due to the no-friction assumption; $\nu\,(\mathbf{e}_2, \mathbf{e}_1)$ is partially restored; different models lead to a total recovery of this elastic property (see WELEMANE and CORMERY [26]); in this case, imposing this total restitution would lead to the following relation:

$$C_2 = 2\alpha \tag{5.5}$$

which is in contradiction with the chosen recovery conditions (except if $\alpha = 0$). However, even if the complete restoration is consequently impossible, in this case it reaches 98% of the initial value.

Some figures regarding generalized elastic moduli for different microcrack related damage models can be found in WELEMANE and CORMERY [26].

5.2. Prediction of a triaxial compression loading path

A triaxial compression simulation with a 20 MPa confinement pressure on the same Vosges sandstone (PECQUEUR [24]) is analyzed in this section.

The stress-strain response is presented in Fig. 6. The three phases are well described:

(i) The response is first elastic, with an elastic limit of −90 MPa.

(ii) The first part of the nonlinear response is due to the growth of microcracks in the medium. The axial stress reaches a maximum of −140 MPa, when the experimental maximum value is −150 MPa; both the axial and lateral strains at the maximal stress level are slightly underestimated.

(iii) The softening phase occurs when damage reaches a critical value. This phase is not shown on the experimental curve due to the lack of information. However, on other simulations (for example with a confinement pressure of 15 MPa), the simulated decrease of axial stress seems to be slower than the experimental one. Nevertheless, as the model does not take into account non-local phenomena, the validity of this inference is questionable.

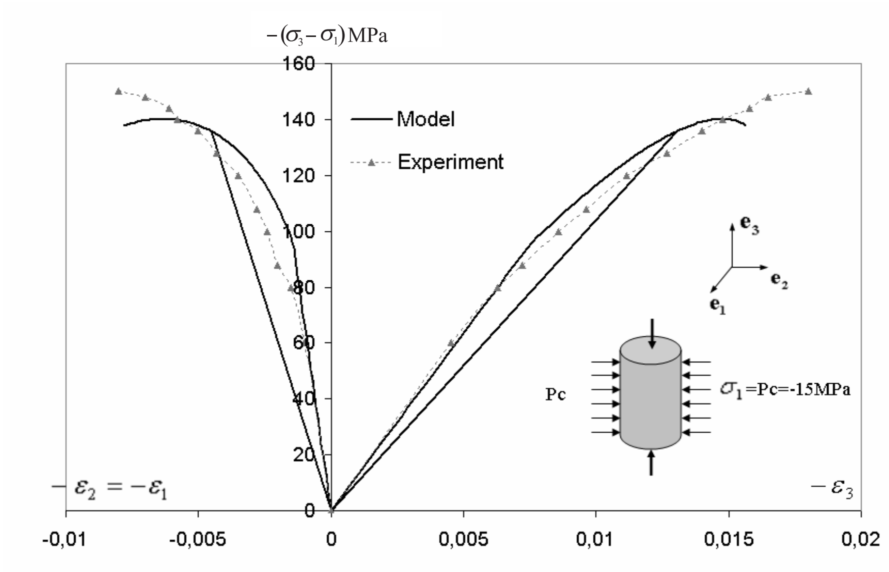

Fig. 6. Stress-Strain response of a Vosges sandstone under triaxial compression with 20 MPa confinement.

Remark 8. Unloading simulation is shown in Fig. 6. As residual effects and dissipative friction are neglected, the curve turns back to the origin. Consideration of dissipative friction and residual effects is commented in Sec. 7.

The simulated damage configuration is a set of vertical (and open) microcracks of normals $\mathbf{e}_1$, $\mathbf{e}_2$, $\dfrac{\mathbf{e}_1+\mathbf{e}_2}{\sqrt{2}}$ and $\dfrac{\mathbf{e}_1-\mathbf{e}_2}{\sqrt{2}}$ with identical densities in the four directions. This configuration is in correlation with experimental considerations presented in Sec. 4.

Due to damage growth, the elastic properties of the material change. The axial Young's modulus progressively decreases; on the contrary, $\nu(\mathbf{e}_3,\mathbf{e}_1)$ increases (Fig. 7). If the qualitative evolutions are in accordance with experimental observations, the increase of Poisson's ratio is questionable, since its value reaches 250% of the initial one. However, as shown in Figs. 8 and 9, both the lateral strain-axial strain response and volumetric dilatancy agree quite well with experimental results, even if these responses depend notably on this property (Poisson's ratio $\nu(\mathbf{e}_3,\mathbf{e}_1)$).

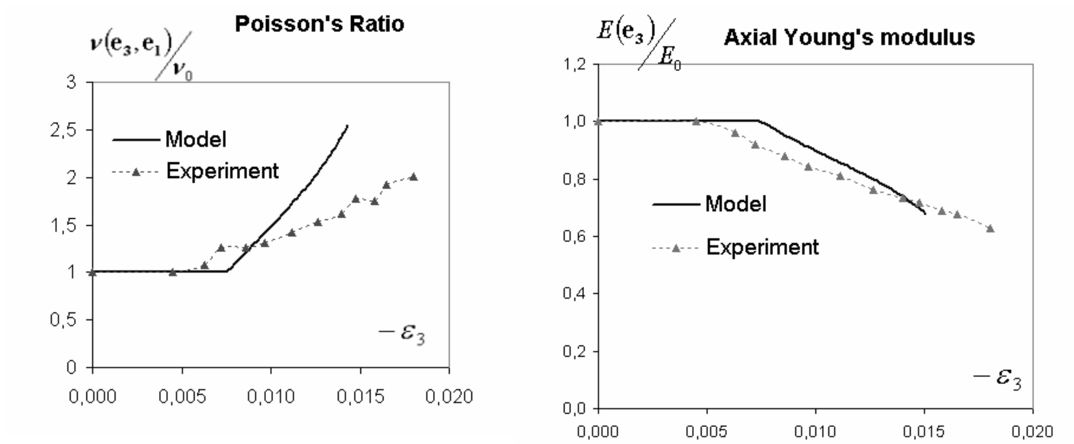

Fig. 7. Evolution of elastic properties.

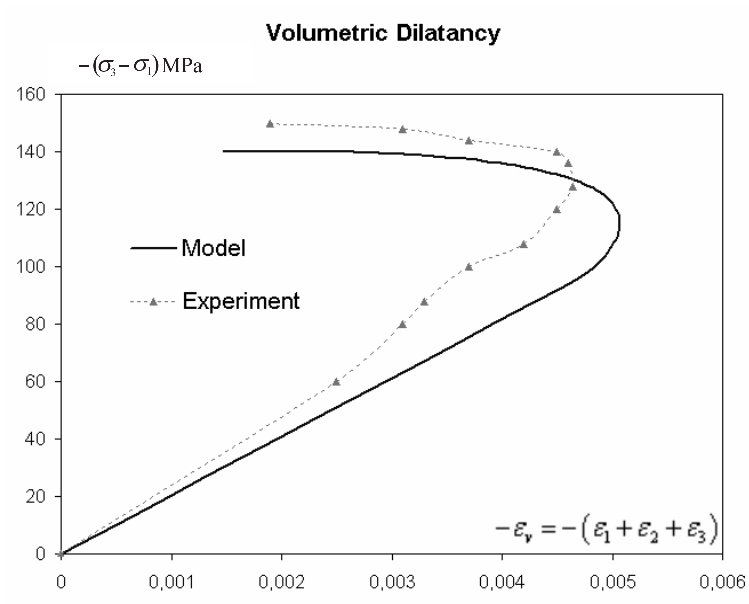

Fig. 8. Volumetric dilatancy for a triaxial loading path.

As said before, the damage configuration is a set of vertical cracks. Figure 10 shows the generalized Young's modulus in the $(\mathbf{e}_1, \mathbf{e}_3)$ plane at one point of the loading path, namely for the axial stress equal –137 MPa. At this stage, the lateral Young's modulus is about 2.5 times lower than the axial Young's modulus.

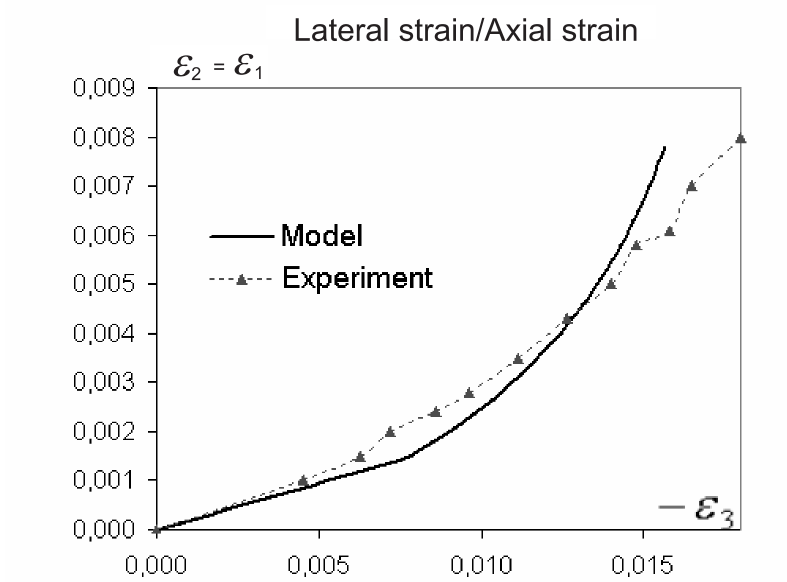

Fig. 9. Lateral strain vs. axial strain response.

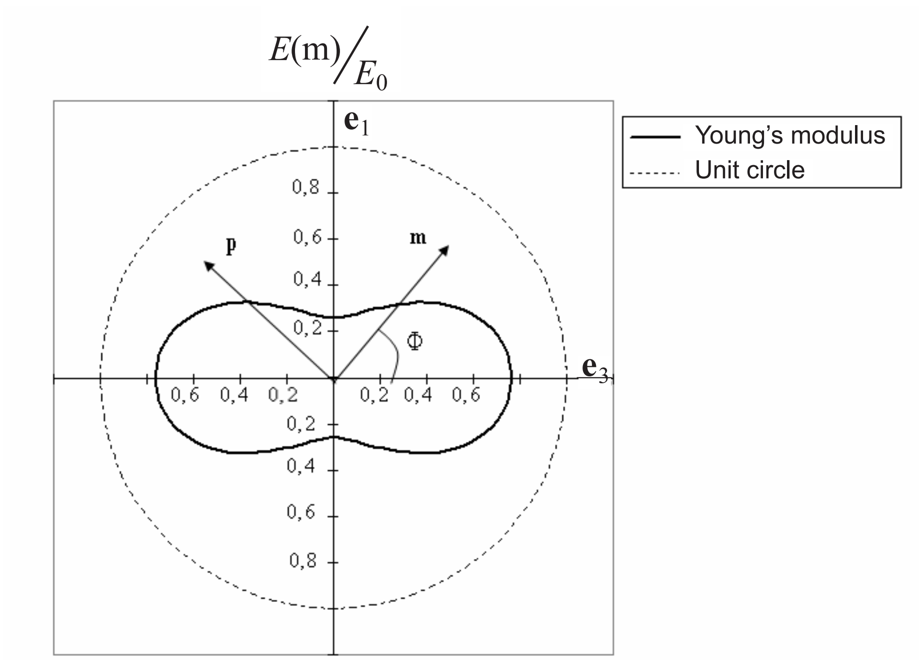

Fig. 10. Generalized Young's modulus normalized by its initial value during a triaxial loading path (at axial stress = –137 MPa).

These results show that the presented model can be considered efficient concerning the most important aspects of quasi-brittle damage: unilateral effect is well taken into account, as shown in the analysis of elastic properties at constant damage configuration; the modelled damage configuration, the volumetric dilatancy and induced anisotropy after a simple loading path are in agreement with experimental results. Further investigation and comparison with experiments, especially concerning the Poisson's ratio, would permit to confirm these aspects.

6. Advantages of the approach

One of the motivations to introduce a discrete anisotropic damage definition was to avoid main inconveniences encountered in earlier approaches. The purpose of this section is to analyze the model under this aspect.

6.1. Strain decomposition

This model does not use any strain decomposition. In Dragon and Halm [7], for example, this decomposition was used to account for induced anisotropy: microcracks grow in directions of positive strain $\boldsymbol{\varepsilon}^+$ (as mentioned in Sec. 4). The damage evolution is proportional to $\boldsymbol{\varepsilon}^+$:

$$\dot{\mathbf{D}} \propto \boldsymbol{\varepsilon}^+ . \tag{6.1}$$

In the presented approach, strain is *naturally* decomposed by orientation tensors $\mathbf{N}_i$; the "$\boldsymbol{\varepsilon}^+$" effect is thus obtained in the following manner:

(i) via the closure condition $\operatorname{tr}(\boldsymbol{\varepsilon}.\mathbf{N}_i) \leq 0$ (cracks are open only if the normal strain is positive),

(ii) by imposing that cracks grow only when they are open.

An uniaxial loading path (tension or compression), in a geometrical two-dimensional case, can illustrate the similarity between the kinetics (6.1) and the evolution law detailed in Sec. 4.

The strain and stress tensors are of the following form for a two-dimensional simulation:

$$\begin{aligned} \boldsymbol{\sigma} &= \begin{bmatrix} \sigma_1 & \\ & 0 \end{bmatrix}, \\ \boldsymbol{\varepsilon} &= \boldsymbol{\varepsilon}_1 \begin{bmatrix} 1 & \\ & -\nu_{12} \end{bmatrix}. \end{aligned} \tag{6.2}$$

The decomposition of the strain tensor into positive and negative parts leads to the following expression of $\boldsymbol{\varepsilon}^+$:

$$\boldsymbol{\varepsilon}^+ = \boldsymbol{\varepsilon}_1 \begin{bmatrix} H(\boldsymbol{\varepsilon}_1) & \\ & \nu_{12} H(-\boldsymbol{\varepsilon}_1) \end{bmatrix}. \tag{6.3}$$

Consequently, damage evolution, according to this model, is the following:

$$\dot{\mathbf{D}} \propto \varepsilon_1 \begin{bmatrix} H(\varepsilon_1) & \\ & \nu_{12} H(-\varepsilon_1) \end{bmatrix}. \tag{6.4}$$

Relation (6.4) shows that under axial tension, only cracks normal to $\mathbf{e'}_1$ (horizontal) will grow; on the contrary, under axial compression, only cracks normal to $\mathbf{e'}_3$ (vertical) will evolve (see Fig. 11a).

The discrete damage definition and the evolution criteria presented in Sec. 4 lead to a similar result.

The first point is to define the four fixed $\mathbf{N}_i$ directions: the $(\mathbf{e}_1, \mathbf{e}_3)$ basis, on which is build the set of $\mathbf{N}_i$, and the $(\mathbf{e}'_1, \mathbf{e}'_3)$ merge: $\mathbf{e}_1 = \mathbf{e'}_1$, $\mathbf{e}_3 = \mathbf{e'}_3$. Relation (2.2) leads to the following set:

$$\begin{aligned} \mathbf{N}_1 &= \mathbf{e}'_1 \otimes \mathbf{e}'_1, \\ \mathbf{N}_5 &= \frac{1}{2}(\mathbf{e}'_1 + \mathbf{e}'_3) \otimes (\mathbf{e}'_1 + \mathbf{e}'_3), \\ \mathbf{N}_8 &= \frac{1}{2}(\mathbf{e}'_1 - \mathbf{e}'_3) \otimes (\mathbf{e}'_1 - \mathbf{e}'_3), \\ \mathbf{N}_3 &= \mathbf{e}'_3 \otimes \mathbf{e}'_3. \end{aligned} \tag{6.5}$$

The crack opening conditions $\operatorname{tr}(\boldsymbol{\varepsilon}.\mathbf{N_i}) \geq 0$ have consequently 3 different forms:

$$\begin{aligned} \boldsymbol{\varepsilon}_1 &\geq 0 && \text{for system 1;} \\ \boldsymbol{\varepsilon}_3 = -\boldsymbol{\nu}_{12}\boldsymbol{\varepsilon}_1 &\geq 0 && \text{for system 3;} \\ \boldsymbol{\varepsilon}_1 + \boldsymbol{\varepsilon}_3 = \boldsymbol{\varepsilon}_1(1 - \boldsymbol{\nu}_{12}) &\geq 0 && \text{for systems 5 and 8.} \end{aligned} \tag{6.6}$$

In compression, only vertical microcracks of normal $\mathbf{e}_3$ (corresponding to system 3) are open and can consequently grow. In addition, the four associated thermodynamic forces are equal (relation (3.14)), so the crack densities are identical (axial symmetry).

In tension, as $0 \leq \nu_{12} \leq 0.5$, microcracks associated with systems 1, 5 and 8 are open and can consequently grow; however, expression (4.1) of thermodynamic force $F_2^{\rho_i}$ leads to the following relations:

$$F_2^{\rho_1} \geq F_2^{\rho_5} = F_2^{\rho_8}. \tag{6.7}$$

Consequently, the microcracks evolve first and faster in direction 1 (horizontal microcracks); in the other directions, the densities are identical (axial symmetry).

The two damage-induced configurations according to the present model are presented in Fig. 11b. In compression, the two damage definitions are thus equivalent. In tension, the main damage configurations (horizontal microcracks) are identical; but the discrete definition adds some cracks oriented at 45° with respect to the loading direction. This added damage direction is experimentally observed as explained in Sec. 4.1.

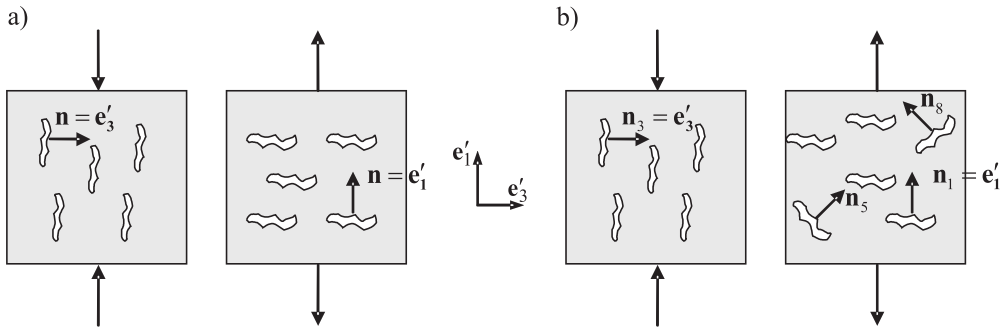

Fig. 11. Simulated damage configuration with strain tensor decomposition a) and discrete damage definition b) under uniaxial tension or compression.

6.2. Dissipation positivity

This model is not standard in the sense of Halphen and Nguyen [21]. The model is written in a non-associated framework. In addition, the thermodynamic forces are split into two parts in Eq. (4.1) and only the second one enters the reversibility domains definition (relation (4.2)). This decomposition has been made to ensure the non propagation of closed cracks. The latter one is a strong hypothesis of the present model; it appears as an acceptable one in view of some experimental observations (Fanella and Krajcinovic [1], Horii and Nemat-Nasser [19] and Ju [20]).

According to expression (6.8) of dissipation $\mathcal{D}$ given below, a sufficient condition for its positivity is to ensure the positivity of each elementary dissipation $\mathcal{D}_i = F^{\rho_i}\dot{\rho}_i$ for a microcrack system:

$$\mathcal{D} = \sum_{i=1}^{9} \mathcal{D}_i = \sum_{i=1}^{9} F^{\rho_i}\dot{\rho}_i \geq 0. \tag{6.8}$$

Equation (4.4) leads to the positivity of $\dot{\rho}_i$, since it is equal to a damage multiplier. Moreover, Eq. (4.5) verifies that $\dot{\rho}_i$ reduces to zero when $\mathrm{tr}(\boldsymbol{\varepsilon}.\mathbf{N}_i) \leq 0$. The sign of $\mathcal{D}_i$ is consequently that of the thermodynamic force F^{ρ_i} when $\mathrm{tr}\,(\boldsymbol{\varepsilon}.\mathbf{N}_i) \geq 0$. In this case, its expression reduces to (from (3.14)):

$$
\begin{aligned}
F^{\rho_i}(\boldsymbol{\varepsilon}_i;\mathbf{N}_i) &= -\alpha\left[tr\left(\boldsymbol{\varepsilon}.\boldsymbol{\varepsilon}\right)-\frac{1}{2}\mathrm{tr}^2(\boldsymbol{\varepsilon})+\mathrm{tr}\left(\boldsymbol{\varepsilon}\right)\ \mathrm{tr}\left(\boldsymbol{\varepsilon}.\mathbf{N_i}\right)\right]-2\beta\mathrm{tr}\left(\boldsymbol{\varepsilon}.\boldsymbol{\varepsilon}.\mathbf{N_i}\right), \\
&= -\alpha h\ (\boldsymbol{\varepsilon};\mathbf{N_i})-2\,\beta\ \ g\left(\boldsymbol{\varepsilon};\mathbf{N_i}\right).
\end{aligned} \tag{6.9}
$$

The second part, namely $g\left(\boldsymbol{\varepsilon};\mathbf{N}_i\right)=\mathrm{tr}\left(\boldsymbol{\varepsilon}.\boldsymbol{\varepsilon}.\mathbf{N}_i\right)$, is unconditionally positive. The first one, namely $h\left(\boldsymbol{\varepsilon};\mathbf{N}_i\right)=\left[\mathrm{tr}\left(\boldsymbol{\varepsilon}.\boldsymbol{\varepsilon}\right)-\frac{1}{2}\mathrm{tr}^2(\boldsymbol{\varepsilon})+\mathrm{tr}\left(\boldsymbol{\varepsilon}\right)\ \mathrm{tr}\left(\boldsymbol{\varepsilon}.\mathbf{N}_i\right)\right]$, needs further investigations.

In the general case, strain $\boldsymbol{\varepsilon}$ (written in its principal axes) and direction $\mathbf{N}_i=\mathbf{n}_i\otimes\mathbf{n}_i$ (with $\|\mathbf{n}_i\|=1$) tensors can be expressed in the following form:

$$
\begin{cases}
\varepsilon=\begin{bmatrix}\varepsilon_1 & & \\ & \varepsilon_2 & \\ & & \varepsilon_3\end{bmatrix}, \\
\begin{cases}
\mathbf{N}_i=\begin{bmatrix}x^2 & x\,y & x\,z \\ x\,y & y^2 & y\,z \\ x\,y & y\,z & z^2\end{bmatrix}, \quad (x,\ y,\ z)\in[0,1]^3 \\
x^2+y^2+z^2=1.
\end{cases}
\end{cases} \tag{6.10}
$$

Definition (6.10) leads to the expression of the investigated part $h\left(\varepsilon;\mathbf{N}_i\right)$ of the thermodynamic force as follows:

$$
\begin{aligned}
h\left(\varepsilon_1,\varepsilon_2,\varepsilon_3;x;y;z\right)=\Bigg[\varepsilon_1^2\left(x^2+\frac{1}{2}\right)+\varepsilon_2^2\left(y^2+\frac{1}{2}\right)+\varepsilon_3^2\left(z^2+\frac{1}{2}\right) \\
-\varepsilon_1\varepsilon_2 z^2-\varepsilon_1\varepsilon_3 y^2-\varepsilon_3\varepsilon_2 x^2\Bigg],
\end{aligned} \tag{6.11}
$$

$h\left(\varepsilon_1,\varepsilon_2,\varepsilon_3;x;y;z\right)$ is a three-variable function with three parameters (x, y and z).

Using the theory of multivariable functions, it can be shown that zero is the minimum value of this function (taken for $\varepsilon_1=\varepsilon_2=\varepsilon_3=0$); $h\left(\varepsilon_1,\varepsilon_2,\varepsilon_3;x;y;z\right)$ is consequently unconditionally positive.

As both $g\left(\boldsymbol{\varepsilon};\mathbf{N}_i\right)$ and $h\left(\boldsymbol{\varepsilon};\mathbf{N}_i\right)$ functions are positive, imposing the condition (6.12) below on material parameters finally ensures the dissipation positivity.

$$
\alpha\le 0,\qquad \beta\le 0. \tag{6.12}
$$

6.3. Continuity and uniqueness of free energy

In this approach, the continuity of the free energy is ensured by relations (3.7) to (3.9): as the stiffness matrix is of rank one, both the free energy w and stress-strain response are continuous.

In addition, thanks to the evolution laws and to the selected orthonormal basis of the Euclidean space $\Re^3$, discretized fixed orientation-tensors $\mathbf{N}_i$ as well as the variables ρ_i have a unique well-defined value. Previously, in the model proposed by Halm and Dragon [6], w was also a continuous function of the set of its arguments, but the damage variable $\mathbf{D}$ could have different values depending on its spectral decomposition, that led to the w non-uniqueness, see Cormery and Welemane [11].

6.4. Closure term

The closure term, which restores some elastic properties at microcrack closure, appears directly using the tensor functions representation theory (Boelher [13]) with the discrete damage definition, while this term had to be somewhat artificially added to those obtained by this theory when the unique damage variable $\mathbf{D}$ was employed. Indeed, Halm and Dragon [6] imposed a complementary fourth-order tensor entity assembled with the eigenvalues and eigenvectors of $\mathbf{D}$ to account for the unilateral effect; a term containing this imposed entity is added to the 'basic' free energy expression and leads to modifications of the stiffness matrix. The same effects on stiffness are here directly obtained in the framework of the discrete definition (via invariant $\mathrm{tr}^2(\boldsymbol{\varepsilon}.\mathbf{N}_i)$), without postulating the existence of a supplementary entity.

7. Conclusion and prospects

A macroscopic and phenomenological anisotropic damage model is presented in this paper. The proposed discrete damage definition, which introduces nine microcrack densities associated with nine *fixed* directions, enables to represent essential phenomena concerning quasi-brittle material behaviour: the induced anisotropic degradation of elastic properties and the dependence of elastic moduli on the microcracks state (open or closed), known as unilateral effect, are notably described.

In addition, this approach avoids some inconveniences encountered by models using the unique second-order tensor variable $\mathbf{D}$ and its spectral decomposition, such as non-uniqueness of the free energy or decomposition of the strain tensor into the positive and negative parts.

However, some experimental verifications of the different assumptions (for example recovery conditions) and of the induced anisotropy (especially regarding the Poisson's ratio) should be further investigated. In addition, its efficiency should be confirmed by testing the model for a number of complex loading paths, in which eigenvectors of the strain tensor do not remain fixed in space.

The enrichment of the model to account for complementary phenomena is the most important prospect.

Dissipative friction on closed microcracks lips leads to the appearance of a blocked energy (Andrieux *et al.* [3]) and residual effects; it will be described by a sliding internal variable, in the spirit of the contribution of Halm and Dragon [27], see also Dragon and Halm [7]. The discrete approach, as it defines fixed directions associated with a closure condition, seems to offer a favourable framework for this purpose.

The interaction between initial and induced anisotropy, essential for example for the Ceramic Matrix Composites, may be modelled by adding fabric tensors in the framework of the tensor functions representation theory (Boehler [13]), as done by Halm *et al.* [28], Dragon and Halm [7] or Gruescu [29]. The fabric tensors $\mathbf{A}_i(\mathbf{a}_i \otimes \mathbf{a}_i)$ indicate the direction of reinforcement of the composite, and the set $\mathbf{N}_i$ indicate damage orientation. Some optimization regarding the set $\mathbf{N}_i$ vs. the set $\mathbf{A}_i$ could allow for further simplification of the advanced theory.

Coupling the initial anisotropy with closure effects would certainly be the most significant perspective of this model.

References

1. D. Fanella, D. Krajcinovic, *A micromechanical model for concrete in compression*, Eng. Fracture Mech., **29**, 1, 49–66, 1988.

2. D. Krajcinovic, *Damage mechanics*, Mech. Mat., **8**, 117–197, 1989.

3. S. Andrieux, Y. Bamberger, J. J. Marigo *A model of microcracked materials for concretes and rocks* [in French], J. de Méc. Théorique et Appliquée, **5**, 3, 471–513, 1986.

4. J.L. Chaboche, *Damage-induced anisotropy: on the difficulties associated with the active /passive unilateral condition*, Int. J. Damage Mech, **1**, 149–171, 1992.

5. A. Dragon, F. Cormery, T. Désoyer and D. Halm., *Localized failure analysis using damage models*, Localization and bifurcation theory for soils and rocks, R. Chambon et coll. [Eds.], Balkema, Rotterdam, 127–140, 1994.

6. D. Halm and A. Dragon, *A model of anisotropic damage by mesocrack growth; unilateral effect*, Int. J. Damage Mech., **5**, 384–402, 1996.

7. A. Dragon and D. Halm, *Damage mechanics, some modelling challenges*, Series: AMAS Lecture Notes 9, 139 pages, AMAS Warsaw 2004.

8. I.Carol, K. Willam, *Spurious energy dissipation/generation in stiffness recovery models for elastic degradation and damage*, Int. J. Solids Structures, **33**, 20–22, 2939–2957, 1996.

9. M. Ortiz, *A constitutive theory for the inelastic behaviour of concrete*, Mech. Mat., **4**, 67–93, 1985.

10. J. Ju, *On energy-based coupled elastoplatic damage theories*, Int. J. Solids Structures, **25**, 803–833, 1989.

11. F. Cormery and H. Welemane, *A critical review of some damage models with unilateral effect*, Mech. Res. Com., **29**, 391–395, 2002.

12. J.L. Chaboche., *Development of continuum damage mechanics for elastic solids sustaining anisotropic and unilateral damage*, Int. J. Damage Mech., **2**, 311–329, 1993.

13. J.P. Boehler, *Anisotropic behaviour laws in continuum mechanics* [in French], J. Méca., **17**, 153–190, 1978.

14. P. Germain, Q.S. Nguyen and P. Suquet, *Continuum thermodynamics*, J. Applied Mechanics, **50**, 1010–1020, 1983.

15. M. Kachanov, *Effective elastic properties of cracked solids: critical review of some basic concepts*, ASME Appl. Mech. Rev., **45**, 8, 304–335, 1992.

16. A. Curnier, Q. He. and P. Zysset, *Conewise linear elastic materials*, J. Elasticity, **37**, 1–38, 1995.

17. M. Sibaï, L. Dormieux, V. Pensée. and D. Kondo, *Effects of microcracking on rocks poroelasticity: experimental study and theoretical analysis* [in French], Proc. French Congress of Mechanics XVI, 2003.

18. V. Pensée and D. Kondo, *A 3-D micromechanical analysis of damage by mesocracking* [in French], Comptes Rendus de l'Académie des Sciences - Series IIB - Mechanics, **329**, 4, 271–276, 2001.

19. H. Horii, S. Nemat Nasser, *Compression-induced microcrack growth in brittle solids : Axial splitting and shear failure*, J. Geophysical Research, **90**, B4, 3105–3125, 1985.

20. J. Ju, *On two-dimensional self-consistent micromechanical damage models for brittle solids*, Int. J. Solids and Structures. **27**, 2, 227–258, 1991.

21. B. Halphen and Q.S. Nguyen, *On generalized standard materials* [in French], J. Méca., **14**, 1, 39–63, 1975.

22. J.P. Deflandre, O. Vincké, E. Rebut, *Contribution of the acoustic emission analysis to the interpretation of the uniaxial compressive test*, Proc. 35^{th} U.S. Symposium on Rock Mechanics, Daemen & Schultz, 867–872, 1995.

23. M. Hayes, *Connexions between the moduli for anisotropic elastic materials*, J. Elasticity, **2**, 2, 1972.

24. G. Pecqueur, *Experimental study and modelling of a chalk and a sandstone in torsion* [in French], PhD Thesis, University Lille I, 1995.

25. M. Kachanov, *Elastic solids with many cracks and related problems*, Adv. Appl. Mech., Vol. 30, Hutchinson J. and Wu T. [Eds.], Academic Press, 259–445, New York 1993.

26. H. Welemane and F. Cormery, *Some remarks on the damage unilateral effect modelling for microcracked materials*, Int. J. Damage Mech, **11**, 65–86, 2002.

27. D. Halm, A. Dragon, *An anisotropic model of damage and frictional sliding for brittle materials*, Eur. J. Mech., A/Solids, **17**, 3, 439–460, 1998.

28. D. Halm, A. Dragon and Y. Charles, *A modular damage model for quasi-brittle solids: interaction between initial and induced anisotropy*, Arch. Appl. Mech., **72**, 498–510, 2002.

29. C. Gruescu., *A scale transition approach for damage in anisotropic materials: application to quasi-brittle matrix composites* [in French], PhD Thesis, University Lille I, 2004.

Received June 27, 2005; revised version February 2, 2006.